Random Field systems

Alexander K. Hartmann
hartmann@theorie.physik.uni-goettingen.de
Institut für theoretische Physik, Bunsenstr. 9
37073 Göttingen, Germany
Tel. +49-551-395995, Fax. +49-551-399631

February 10, 2000

Contents

This text introduces a model for a certain class of random magnetic systems. They consist of lattices where the atoms have a small magnetic moment, i.e. a *spin*. Within this model, for neighboring spins it is energetically favorable to point into different directions, that means they interact *antiferromagnetically*. But not all sites of the lattice are occupied by magnetic atoms, one calls the system *diluted*. If such a system is submitted to a external magnetic field it is called *diluted antiferromagnet in a field (DAFF)*.

This class of systems has been studied widely by means of experiments and computer simulations at finite temperature. For analytical calculations another type of system, the so called random-field model, is believed to be equivalent and allows a better treatment. Later a definition of this model will be given as well. Here, we are interested in the low temperature-properties of the systems, especially in the ground states. From the viewpoint of a computational physicist the calculation of ground states of this type of systems belongs to the class of P problems, i.e. the $T = 0$ behavior can be studied up to large system sizes.

At the beginning both models and some basic results are presented. Then it is shown how these systems can be mapped onto networks. It is demonstrated that the maximum flow through such a network is equivalent to the minimum energy of the corresponding system. Next, for pedagogical reasons, a simple algorithm for calculating the maximum flow is presented. Finally, some of the most interesting results, obtained with this algorithm, are shown.

1 Diluted antiferromagnets and random field systems

For diluted antiferromagnets with a high anisotropy the spins are usually oriented along one axis. Thus, they can take only two directions, called "*up*" and "*down*".

The *Ising model* is suited very well to represent such kind of system. It is a d-dimensional lattice of Ising spins $\sigma_i = \pm 1$. For a DAFF, they interact antiferromagnetically with their neighbors. To describe the dilution a second variable $\epsilon_i = 0, 1$ is introduced. An empty site is represented by $\epsilon = 0$ while $\epsilon = 1$ holds for a site occupied by a spin. Additionally an external magnetic field B can act on the spins. The energy of a diluted antiferromagnet in a field is given by

$$H = \sum_{\langle i,j \rangle} J \epsilon_i \epsilon_j \sigma_i \sigma_j - B \sum_i \epsilon_i \sigma_i \qquad (1)$$

The strength of the interaction is denoted with $J > 0$. The sum $\langle i,j \rangle$ runs over pairs of nearest neighbors. Here only simple cubic lattices are considered. Since physical properties depend on the values of the ϵ_i one has to implement *quenched disorder*. This means that one draws a set $\{\epsilon_i\}$ of random numbers, here we will consider $\epsilon_i = 0, 1$ with equal probability. A system with a certain choice of the values $\{\epsilon_i\}$ is called a *realization* of the disorder. These values remain fixed for the calculations of physical quantities. Since the result of each calculation depends on the choice of the $\{\epsilon_i\}$, one has to repeat the process several times and average the results over many realizations. It turns out that for random systems the results vary strongly from realization to realization. Therefore one needs many of them to obtain reliable results.

What can we expect for the behavior of this model? In zero field and with zero temperature the ground state, i.e. the state with the lowest energy is taken. Therefore, in (1) configurations $\{\sigma_i\}$ are favorable where neighboring spins take different orientations, because their contribution to the energy $J\sigma_i\sigma_j = -J$ turns out to be negative. It means that, apart from the fact that not all lattice site are occupied, the system can be divided into two sublattices, which penetrate each other in checkerboard fashion. On one of these sublattices all spins point into one direction (say up), while the spins of the other sublattice are oriented in the opposite way. In Fig. 1 an example of a $d = 2$ dimensional diluted antiferromagnet at $B = T = 0$ is shown. In higher dimensions the model behaves similar, but it is more difficult to draw.

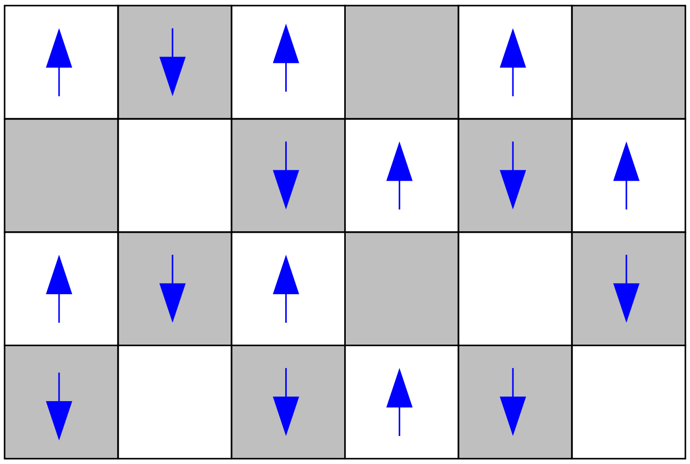

Figure 1: Two-dimensional diluted antiferromagnet without external field. The spins are indicated by arrows. Shown is a ground state $T = 0$. Please note that the configuration which is obtained by reversing all spins is a ground state as well.

By increasing the temperature, the DAFF is driven away from the ground state. This means the spins start to fluctuate thermally. When some critical temperature is reached the system becomes paramagnetic. Also by increasing the magnitude of the external magnetic field, the antiferromagnetic order is disturbed. For large values of B, especially if $|B| > 2dJ$, all spins point into the direction of the field (at $T = 0$).

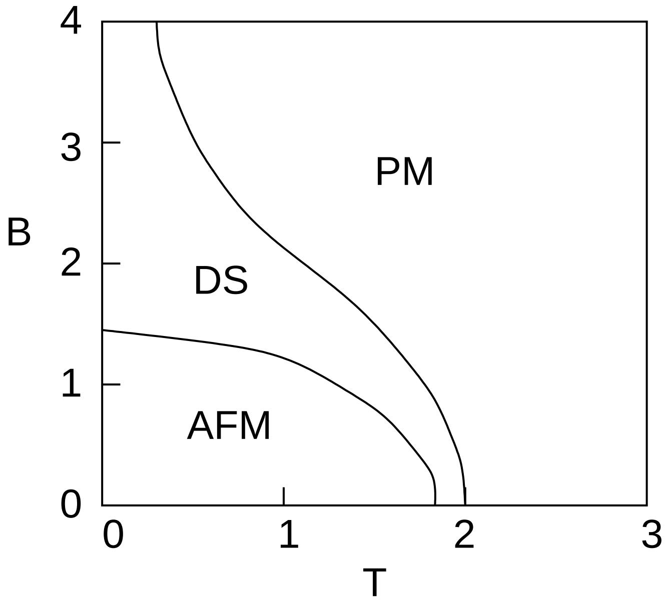

Figure 2: Schematic phase diagram of the DAFF in the B-T plane, obtained by MC simulation [5]. Three regions can be identified: antiferromagnetic (AFM), domain state (DS) and paramagnetic (PM).

These expectations can be recovered in the schematic phase diagram of the three-dimensional DAFF model (50% dilution) which is shown in Fig. 2. It was measured by means of Monte-Carlo simulations at finite temperature T [4, 5]. The ordered phase for low temperatures and low fields was established by evaluating the staggered magnetization

$$a = \frac{1}{N} \sum_i (-1)^{x+y+z} \sigma_i \; . \tag{2}$$

Here, x, y, z are the spatial coordinates of spin i. This order parameter accounts for the fact that in the presence of order the two penetrating sublattices have opposite magnetizations. Therefore $a = 1$ holds for antiferromagnetic order on a cubic lattice. The transition of the so called domain state (DS) to the disordered phase is established in the following way: for a given field B the system is initialized in an ordered state at $T = 0$ and the MC simulation starts. Then, slowly the temperature is increased, here up to $T = 2.5$. This process is called field heating (FH). Then the temperature is slowly decreased again (FC=field cooling). Now, the system is not able find the way back to the starting configuration. This can be seen by recording the staggered magnetization. At some temperature $T_{irr}(B)$ the FH and FC curves begin to deviate from each other. This is called an onset of *irreversibility*. The line which separates the PM and the DS regions in Fig. 2 is just T_{irr} as a function of B. Please note that the value of $T_{irr}(B)$ defined in this fashion depends on the dynamics, i.e. on the heating-/cooling rate. A more detailed study has shown that the DS region can be characterized by large fractal domains penetrating the system.

The behavior of true diluted antiferromagnets agrees very well with these computer simulations. But it is relatively hard to treat this model by means of an analytical approach. As a consequence usually a different model is investigated. The basic idea is to look at the local field $H_i = \sum_j \epsilon_j \sigma_j + B$ which acts on each local spin σ_i. Since the values of the ϵ_j are random, the local fields are, for fixed orientations of the neighbors σ_j, random variables as well. Thus, a system with similar behavior is expected to be obtained if one studies a model without dilution but with the presence of a site-dependent *random field.* An experimental realization of a random-field system is not know. But this kind of model is easier to treat analytically, because the randomness influences only one spin directly. Later we will see that indeed the behavior of this model agrees remarkably with that of the diluted antiferromagnet. The definition of the model is as follows.

A random field Ising magnet (RFIM) is given by a d-dimensional lattice of Ising spins $\sigma_i = \pm 1$ which interact ferromagnetically with their nearest neighbors. On each spin acts a local random magnetic field B_i. The system has the following Hamilton function

$$H = -\sum_{\langle i,j\rangle} J\sigma_i\sigma_j - \sum_i B_i\sigma_i \qquad (3)$$

The sum $\langle i,j\rangle$ runs over pairs of nearest neighbors. $J > 0$ denotes the magnitude of the interaction. Here only simple cubic lattices are considered. The local magnetic fields are drawn independently from a probability distribution $p(B)$. Again, one has to treat several realizations $\{B_i\}$ of the disorder, calculate physical properties for each realization and then take an average. Usually either a bimodal or a Gaussian distribution are used to draw the random realizations. In the case of a bimodal distribution the local fields take one of two values $B_i = \pm\Delta$ with equal probability. For the Gaussian case arbitrary fields are allowed. The probability density functions are

$$\begin{aligned} p_{\pm}(B) &= 0.5\delta(B-\Delta) + 0.5\delta(B+\Delta) &(4)\\ p_G(B) &= \frac{1}{\sqrt{2\pi\Delta^2}}\exp\left(\frac{B^2}{2\Delta^2}\right) &(5)\end{aligned}$$

The parameter Δ, the width of the distribution, is a measure for the strength of the disorder. For $\Delta = 0$ a pure ferromagnet is obtained. Roughly estimated, the RFIM behaves similar as the DAFF. For low temperatures and low fields the system exhibits a ferromagnetic long range order. For large temperatures the system becomes paramagnetic. By increasing the strength Δ of the random fields, the spins tend to be oriented along the direction of the field. If $|B_i| > 2dJ$ spin i is fixed (at $T = 0$). But at zero temperature for intermediates values of the field a peculiar behavior of the RFIM appears, similar to the DS phase of the diluted antiferromagnet. This region of the phase diagram can be studied by means of ground state calculations. The basic idea of the method for obtaining the ground states is explained in the next section.

2 Transformation to a graph

Now it is shown that for a given RFIM an equivalent network can be constructed such that the maximum flow through the network is equal to the ground-state energy of the RFIM. This transformation was introduced by Picard in 1975 [9]. Additionally, the orientations of the spins in a ground state can be easily constructed from the flow values the network takes. In case that the ground state is degenerate, all ground states can be obtained by a subsequent calculation. This case is treated in [17]

It is more instructive to start with a network and to show how it can be transformed into a RFIM. Let $N = (G, c, s, t)$ a network, where $G = (V, E)$ is a directed graph which has $n+2$ vertices, $c : V \times V \to \mathcal{R}_0^+$ are the capacities of the edges $(i,j) \in E$, with $c(i,j) = 0$ if $(i,j \notin E)$. The vertices $s,t \in V$ are the source and the sink of the network, respectively. For convenience, we use $V = \{0, 1, \ldots, n, n+1\}$ where $s \equiv 0$ and $t \equiv n+1$, and the notation $c_{ij} \equiv c(i,j)$. The vertices in $V \setminus \{s,t\}$ are called *inner* vertices. Edges connecting only inner vertices are also called inner edges.

As we have seen, a network can be interpreted as a system of pipes connecting the source with the sink. Now, assume that the network should be divided into two pieces in a way that the source and the sink are separated. You can think of a pipeline system and a group of terrorists who like to prevent the oil from being transported to the refinery. Mathematically, this separation is a (s,t)-*cut* $(S, \overline{S})$ which has the following properties:

- $S \cup \overline{S} = V$
- $S \cap \overline{S} = \emptyset$
- $s \in S$
- $t \in \overline{S}$

Usually, we denote the elements of S *left* and the elements of $\overline{S}$ *right* of the cut. In Fig. 3 an example network with 5 nodes and 6 edges is shown.

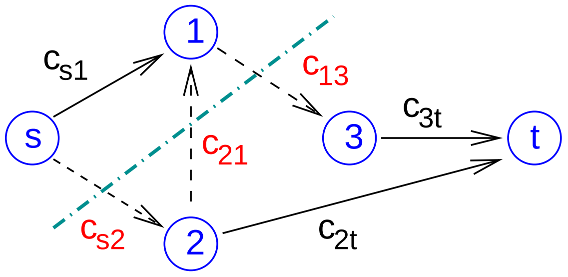

Figure 3: A graph with 3 inner vertices 1,2,3. A cut $(S, \overline{S}) = (\{s,1\}, \{2,3,t\})$ is represented by a dashed-dotted line. The capacity of the cut is $C(\{s,1\}, \{2,3,t\}) = c_{s2} + c_{13})$. The edge $(1,2)$ does not contribute to the cut, because it is oriented in the opposite direction to the cut.

Since the amount of work (or TNT) to remove a pipeline grows with its capacity, the terrorist are interested in the capacity of the pipes they have to remove. These are exactly the pipes which go from S to $\overline{S}$, that means from left to right. We say these pipes/edges *cross* the cut. Edges in the opposite direction cannot contribute to a flow from the source to the sink, thus they are disregarded. The sum of the capacities of these edges is called the *capacity* $C(S, \overline{S})$ of the cut

$$C(S, \overline{S}) = \sum_{i \in S, j \in \overline{S}} c_{ij} \,. \tag{6}$$

In the example presented in Fig. 3 the capacity of the cut is $C(S, \overline{S}) = c_{s2} + c_{13}$. The edge $(1,2)$ does not contribute, since it leads from right to left.

The basic idea to represent a Hamiltonian by a network is to represent a cut by a binary vector $\underline{X} = (x_0, x_1, \ldots, x_n, x_{n+1})$ with

$$x_i = \begin{cases} 1 & i \in S \\ 0 & i \in \overline{S} \end{cases} \tag{7}$$

For an (s,t)-cut the values of $x_0 = 1$ and $x_{n+1} = 0$ are fixed. An edge (i,j) goes from left to right of the cut only if $x_i = 1$ and $x_j = 0$. Therefore, the formula for the capacity of a cut can be rewritten in the following way (all sums run from 0 to $n+1$):

$$\begin{aligned} C(\underline{X}) \equiv C(S,\overline{S}) &= \sum_{i,j} x_i(1-x_j)c_{ij} \\ &= -\sum_{i,j} c_{ij}x_ix_j + \sum_i \left(\sum_j c_{ij}\right) x_i \end{aligned} \tag{8}$$

Here, it can be seen already that the structure of the formula resembles the energy functions for the random field system: it consists of a linear and a quadratic term. To make to correspondence complete, the values of the source and the sink $x_0 = 1, x_{n+1} = 0$ have to be inserted, additionally $c_{ii} = 0 \quad \forall i$ is assumed. For didactic reasons, the capacities involving the source 0 or the sink $n+1$ are written as extra terms. One obtains:

$$C(x_1,\ldots,x_n) = -\sum_{i,j=1}^{n} c_{ij}x_ix_j + \sum_{i=1}^{n}\left(-c_{0i} + c_{i,n+1} + \sum_{j=1}^{n} c_{ij}\right) x_i + \sum_{i=1}^{n} c_{0i} + c_{0,n+1} \tag{9}$$

The last slight difference to a Hamiltonian is that the capacity is given in terms of zero-one variables $x_i = 0,1$ while a spin may take $\sigma_i = \pm 1$. Thus, one can identify $x_i = 0.5(\sigma_i + 1)$. In the Hamiltonian the sum runs over all bonds, while for $C(x_1,\ldots,x_n)$ each pair of vertices appears twice in the quadratic term. Thus, the identity $\sum_{ij} c_{ij} = \sum_{i<j}(c_{ij} + c_{ji})$ is used. In the final formula all sums run from 1 to n:

$$\begin{aligned} C(\sigma_1,\ldots,\sigma_n) &= -\sum_{i<j} \frac{1}{4}(c_{ij}+c_{ji})\sigma_i\sigma_j \\ &\quad + \sum_i \left(-\frac{1}{2}c_{0i} + \frac{1}{2}c_{i,n+1} + \frac{1}{4}\sum_j (c_{ij} - c_{ji})\right)\sigma_i \\ &\quad + \frac{1}{4}\sum_{i<j}(c_{ij}+c_{ji}) + \frac{1}{2}\sum_i (c_{0i} + c_{i,n+1}) + c_{0,n+1} \end{aligned} \tag{10}$$

This formula represents a system which has $n+2$ vertices: one source, one sink and n (inner) vertices, one for each spin σ_i. The model is slightly more general than the system represented by the Hamiltonian in (3). Thus, formula (10) can be compared with an energy function of the form ($\epsilon_i = 0,1$)

$$H = -\sum_{i<j} J_{ij}\epsilon_i\epsilon_j\sigma_i\sigma_j - \sum_i B_i\epsilon_i\sigma_i\,. \tag{11}$$

This is a diluted random field system with bonds of variable strength. No we want to chose the capacities c_{ij} in a way, that this system is represented by a network. By comparison with (10) we find $c_{ij} + c_{ji} = 4J_{ij}\epsilon_i\epsilon_j$ for $i,j \in 1,\ldots,n$. Since for a network only non-negative capacities are allowed, the bond values have to be non-negative as well. Both c_{ij} and c_{ji} appear in the equality, so there is some freedom of choice. We chose that non-zero capacities shall be present only for edges (i,j) with $i<j$. Consequently we obtain $i,j \in 1,\ldots,n$:

$$c_{ij} \equiv \begin{cases} 0 & \text{if } i \geq j \\ 4J_{ij}\epsilon_i\epsilon_j & \text{else} \end{cases} \tag{12}$$

Now we are left with the capacities $c_{0i}, c_{i,n+1}$ $(i = 1, \ldots, n)$ and $c_{0,n+1}$. Next, the linear terms in (10) and (11) have to be compared. Defining

$$w_i \equiv -2B_i\epsilon_i - \frac{1}{2}\sum_j (c_{ij} - c_{ji}) \tag{13}$$

we obtain $-c_{0i} + c_{i,n+1} = w_i$. The value of w_i may be positive or negative. Again, all capacities have to be non-negative. Therefore, we get

$$\begin{aligned} c_{0i} \equiv 0 \quad & c_{i,n+1} \equiv w_i \qquad \text{if} w_i > 0 \\ c_{0i} \equiv -w_i \quad & c_{i,n+1} \equiv 0 \qquad \text{else} \end{aligned} \tag{14}$$

Finally, since the sum of the constant terms in (10) must vanish, we obtain

$$c_{0,n+1} \equiv -\frac{1}{4}\sum_{i<j}(c_{ij} + c_{ji}) - \frac{1}{2}\sum_i (c_{0i} + c_{i,n+1}) \tag{15}$$

The capacity $c_{0,n+1}$ of the edge may be positive or negative. But in this case it does not matter, since this edge crosses every (s,t)-cut of the network. Consequently, it can be removed from the network at the beginning. Later, after the capacity of a cut has been obtained, the value of $c_{0,n+1}$ has to be added to get the energy of the corresponding system.

Please note that the Hamiltonian (11) describes a DAFF as well, if $J_{ij} = -J < 0$ and $B_i = B$ are chosen. In this case the couplings are not positive, i.e. a direct transformation to a network with positive capacities is not possible. But in the case of a simple cubic (or square) lattice, there is a solution. On performs a *gauge transformation* by introducing new spin variables $\sigma_i^{'} = (-1)^{x+y+z}\sigma_i$, where x, y, z are the spatial coordinates of spin i. This transformation multiplies every second spin with minus one, thus all bonds become ferromagnetic. The resulting Hamiltonian describes a diluted ferromagnet with staggered field $B_i = (-1)^{x+y+z}B$. Please note that this kind of transformation does not work for all lattice types, for example triangular lattices.

To summarize, for a system defined by the energy function (11) an equivalent network can be constructed by creating a graph which has one vertex for each spin and additionally a source and a sink. The capacities of the edges are chosen by performing the steps given through equations (12,14,15). Then, every configuration of the system corresponds to a cut in the network ($\sigma_i = 2x_i - 1$) and the energy $H(\sigma_1, \ldots, \sigma_n)$ is equal to the capacity $C(x_1, \ldots, x_n)$ of the corresponding cut.

Since we are interested in ground states, a minimum of the energy is to be obtained. Consequently, we are looking for a *minimum cut* that is a cut among all cuts which has minimum capacity. Such a cut cannot be obtained directly, but it is related to the flow going through the network. Each flow must pass the edges crossing an arbitrary cut, especially the minimum cut. Therefore, the minimum cut capacity is an upper bound for the flow. On the other hand, it can be shown that the maximum flow which is possible is indeed given by the capacity of a minimum cut. The proof was found by Ford and Fulkerson in 1956 [10]. Versions of the proof which are more instructive can be found in [7, 8]. Along with the proof a simple method for finding the maximum flow was introduced. After constructing an equivalent network such a technique has to be applied to find a ground state of a random field Ising system. The Ford-Fulkerson algorithm and an extension of it are presented in the next section.

But before we proceed with the algorithms, as an example, we look at a small random field system, which is shown in Fig. 4. There are four spins arranged in a square, neighbors interact via ferromagnetic interactions of strength $J = 1$. The local fields have the values $B_1 = 0$, $B_2 = -2\Delta$, $B_3 = 2\Delta$, and $B_4 = 0$. Even for this tiny system many different effects, depending on the magnitude of Δ, can be studied.

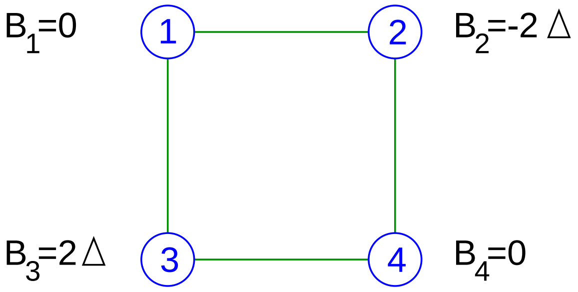

Figure 4: A small random field Ising magnet. It contains 4 spins coupled via ferromagnetic interactions (J_{12} =J_{13} =J_{24} =J_{34} = 1). The local fields have the magnitudes $B_1 = 0$, $B_2 = -2\Delta$, $B_3 = 2\Delta$, and $B_4 = 0$.

Now, an equivalent network is constructed. It contains $n = 4$ inner nodes, one for each spin, and additionally one source 0 and one sink $n + 1 = 5$. We start by setting the capacities of the inner nodes. According (12) we get

$$\begin{aligned} c_{12} &= 4J_{12} = 4 \\ c_{13} &= 4 \\ c_{24} &= 4 \\ c_{34} &= 4 \\ c_{ij} &= 0 \text{ for all other cases } 1 \leq i, j \leq 4 \end{aligned} \tag{16}$$

These values do not depend on the strength of the local magnetic fields. But they enter the expressions for the auxiliary values w_i, see (13)

$$\begin{aligned} w_1 &= -2B_1 - \frac{1}{2}\sum_s (c_{ij} - c_{ji}) \\ &= -2 \times 0 - \frac{1}{2}(c_{12} + c_{13}) \\ &= -4 \\ w_2 &= -2B_2 - \frac{1}{2}(-c_{12} + c_{24}) \\ &= 4\Delta \\ w_3 &= -4\Delta \\ w_4 &= 4\,. \end{aligned} \tag{17}$$

At first the case $\Delta = 0$ is investigated. Thus, no magnetic field acts on the spins. A ferromagnetically ordered ground state is to be expected, thus all spins point up or all spins pointing down at $T = 0$. Since each bond contributes an amount of -1 to the energy, the total ground state energy sums up to $E_0 = -4$. This behavior can be extracted from the corresponding network as well. By setting $\Delta = 0$ in (17) we obtain $w_1 = -4$, $w_2 = 0$, $w_3 = 0$, and $w_4 = 4$. According to (14) the capacities of the edges connecting the inner vertices to the source and the sink are

$$\begin{array}{ll} c_{01} = 4 & c_{15} = 0 \\ c_{02} = 0 & c_{25} = 0 \\ c_{03} = 0 & c_{35} = 0 \\ c_{04} = 0 & c_{45} = 4\,. \end{array} \tag{18}$$

The capacity of the phantom-edge connecting source and sink evaluates according

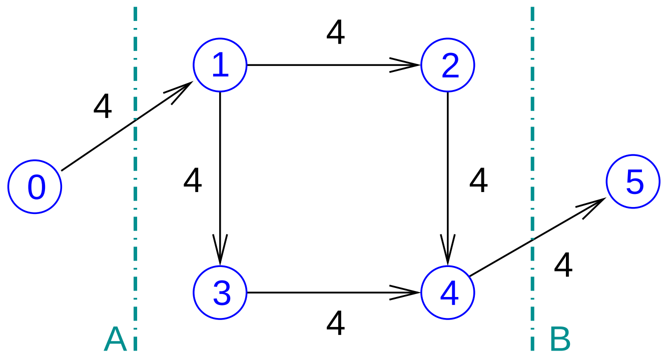

Figure 5: The network obtained for the system from Fig. 4 for the case $\Delta = 0$. Vertex 0 is the source and vertex 5 the sink. The numbers next to the edges denote their capacities.

(15) to c_{05} =$-0.25(4+4+4+4) - 0.5(4+0+0+4)$ =-8. The final network is presented in Fig. 5. The network allows for two minimum $(0,5)$-cuts, indicated by dot-dashed lines in the drawing. Both cuts have capacity $C(S,\overline{S}) = 4 + c_{0,5} = -4$ which is indeed equal to the ground state energy obtained above. The cut denoted with an "A" is given by $(S,\overline{S})$ =$(\{0\},\{1,2,3,4,5\})$. This means $x_0 = 1$ and $x_1 = x_2 = x_3 = x_4 = x_5 = 1$. Using $\sigma_i = 2x_i - 1$ $\sigma_i = 1$ for $i = 1,2,3,4$ is obtained. Thus, really all spins are oriented in the same direction. The cut "B" $(S,\overline{S})$ =$(\{0,1,2,3,4\},\{5\})$ corresponds to the configuration where all spins are pointing down.

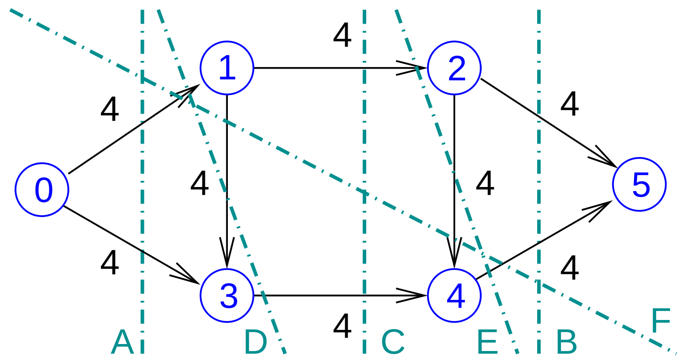

Figure 6: The network obtained for the system from Fig. 4 for the case $\Delta = 1$. Vertex 0 is the source and vertex 5 the sink. The numbers next to the edges denote their capacities.

In the case $\Delta = 1$ the following values for the capacities are obtained:

$$\begin{aligned} c_{01} &= 4 & c_{15} &= 0 \\ c_{02} &= 0 & c_{25} &= 4 \\ c_{03} &= 4 & c_{35} &= 0 \\ c_{04} &= 0 & c_{45} &= 4 \end{aligned}$$
$$c_{05} = -12\,. \tag{19}$$

The resulting network is shown in Fig. 6. Now six different minimum cuts are possible. At the first glance the figure might look somehow complicated. But it is easy to verify that indeed all minimum cuts A to F have capacity $C = 8 + c_{05} = -4$. Please note that only the edges contribute which go from the left side of the cut to the right side. Thus, to the cut F, the edges $(0, 1)$ and $(4, 5)$ contribute to the capacity, but not the edges $(1, 3)$ or $(2, 4)$. The corresponding spin configurations are drawn in Fig. 7. There, the small plus and minus signs state the contributions of the single spins/spin pairs to the total ground state energy. In all 6 cases the ground state energy is $E_0 = -4$, which is again equal to the capacity of all minimum cuts. The six ground states can be described as follows: for two configurations the system is ordered, all spins either point up or all spins point down. In this two ordered configurations one of the spins 2/3 is oriented against its local field. The remaining four ground states are characterized by the fact that spins 2,3 point into the direction of their local magnetic fields and the remaining spins can be either up or down independently.

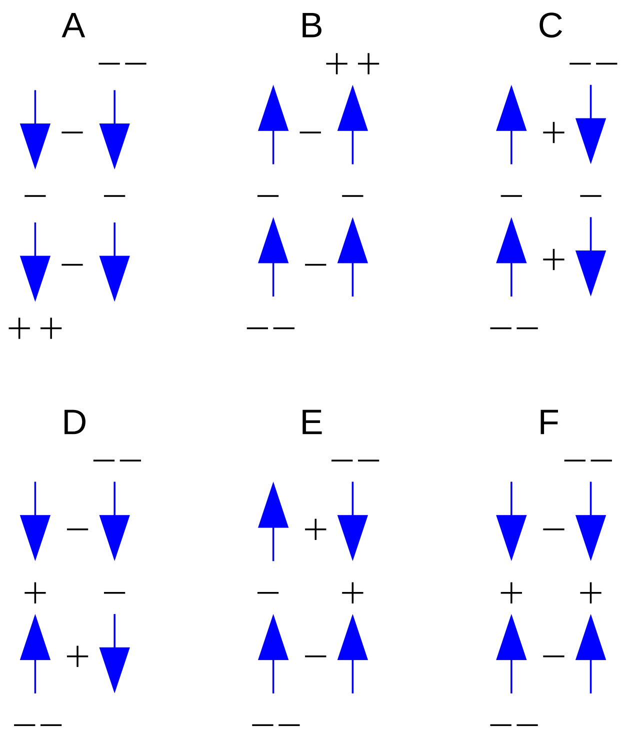

Figure 7: Ground states of the RFIM shown in Fig. 4 for the case $\Delta = 1$. The system has 6 ground states with the same energy $E_0 = -4$. The arrows indicate the orientations of the spins. The plus and minus symbols represent contributions to the ground-state energy.

The example graphs we have presented here, will also be used in the next section to elucidate how the algorithms for calculating maximum flows work.

3 Simple maximum flow algorithms

In this section two algorithms for calculating the maximum flow in a network from the source to the sink are given. At the beginning a description of the historically first method is given which was invented by Ford and Fulkerson in 1956 [10]. Then it is shown by a simple example that this technique has no polynomial bound in the number of nodes and edges, thus it is not suitable in practice. Finally, a variant of the Ford-Fulkerson algorithm, developed in 1972 by Edmonds and Karp [11] is explained, which indeed has a polynomial time complexity. As usual, the way the algorithms work are illuminated by giving sample runs. A compact description of the methods explained here along with proofs for correctness and time-complexity of the algorithms can be found in [13].

Let $N = (G, c, s, t)$ a network, where $G = (V, E)$ is a directed graph which has $n + 2$ vertices, $c : E \rightarrow \mathcal{R}_0^+$ are the capacities of the edges $(i, j) \in E$ and $s, t \in V$ are the source and the sink, respectively. Let f be a flow in N. i.e. f_{ij} denotes the flow from vertex i to vertex j. Please remember that $f_{ij} = -f_{ji}$ and the that flow is conserved in all vertices except the source and the sink. It is assumed that all capacities are non-negative integer (or rational) values. The aim is to find the maximum flow from the source to the sink.

The basic idea of the Ford-Fulkerson algorithm is to start with an empty network and to try to push additional flow from the source to the sink. This is done by searching for paths along which the flow can be increased, they are called *augmenting paths*. If no such path is found, the algorithm stops and the maximum flow has been found.

But for each single edge, the flow through the edge is not always increased or remains the same. Sometimes it is necessary to decrease the flow in some edges, to increase the total flow through the network. This case appears, when some amount of flow is redirected within the graph. To treat this redirection process efficiently the notion of a *residual network* is useful. The residual network R (often called *residual graph*) for network N and flow f has the same vertices like the graph G. It contains edges with nonzero capacities r_{ij} whenever in G with given flow f it is possible to increase the flow along edge (i, j). Please note that it is also possible to increase a negative flow in (i, j) by decreasing the flow in the reverse edge (j, i). Formally R is defined as follows: $R = (G^{'}, r, s, t)$, $G^{'} = (V, E^{'})$ with

$$r_{ij} \equiv c_{ij} - f_{ij} \, . \tag{20}$$

The graph $G^{'}$ contains directed edges (i, j) for all nonzero capacities $r_{ij} > 0$. Please note that in the residual graph two vertices (i, j) may be connected by two edges (i, j) and (j, i).

The Ford-Fulkerson algorithm reads as follows

algorithm ford-fulkerson(N)
begin
    Intially set $f_{ij} := 0, f_{ji} := 0$ for all $(i, j) \in E$;
    do
        construct residual network R with capacities r_{ij};
        if there is an augmenting path from s to t in $G^{'}$ **then**
        begin
            Let $r_{\min}$ the minimum capacity of r along this path;
            Increase the flow in N along the path by a value of $r_{\min}$;
        end

until no such path from s to t in G' is found;
end

For each augmenting path the edge with the smallest capacity is a bottleneck. This is the reason why the flow along the path can be increased only by the amount of the minimum capacity $r_{\min}$. The augmenting path can be constructed using a breadth-first search. I.e. beginning at the source iteratively neighboring vertices are visited which have not been visited before. During this search at each vertex i the predecessor in the actual path and the minimum residual capacity $r_{\min}(i)$ along the path up to i are stored. In this way each vertex which is connected to the source is visited exactly once. If an augmenting path is found, i.e. if the sink has been visited during the breadth-first search, the flow can be augmented directly by starting at the sink. Iteratively the predecessor is visited and the flow increased by $r_{\min}(t)$ until the source is reached again.

Please note that the algorithm may not converge to the true maximum flow if the capacities are irrational, an example is given in [12].

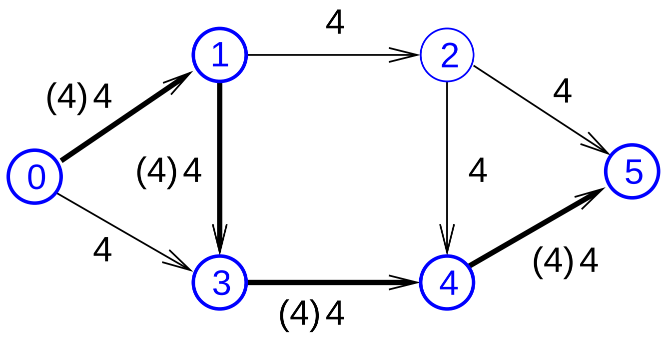

Figure 8: Initial residual network of small random field system. An augmenting path is highlighted. The values next to the edges denote the residual capacities. The embraced values state the amount of flow which can be pushed along the augmenting path.

As an example we investigate how the algorithm calculates the maximum flow through the network given in Fig. 6. At the beginning the flow is empty, so the residual network is equal to the original network. A possible augmenting path from the source 0 to the sink 5 is given by the vertices 0, 1, 3, 4, 5. Each edge along the path has (residual) capacity 4, thus it is possible to increase the flow along the path by this value. The residual graph is shown in Fig. 8, the augmenting path is highlighted. The values in braces next to the edges state the amount of additional flow which can be pushed through each edge along the augmenting path. In this case the resulting original network with the flow after the augmentation looks the same.

For the second iteration, again the residual network has to be calculated. Now, for example in edge $(0,1)$ the flow $f_{01} = 4 = c_{01}$ is present. That means that the residual capacity in direction $(0,1)$ is $r_{01} = c_{01} - f_{01} = 0$, but for the reversed direction a value of $r_{10} = c_{10} - f_{10} = 0 - (-4) = 4$ is obtained. The complete residual network is shown in Fig. 9. In this case only one augmenting path is feasible: 0,3,1,2,5. The capacity of this path is 4. Please note that by augmenting the flow through edge $(3,1)$ in the residual graph, in the original graph the flow through edge $(1,3)$ is decreased. The resulting total flow for the graph is displayed in Fig. 10. Now both edges $(0,1)$ and $(0,3)$ are satisfied. As a consequence, in the corresponding residual graph $r_{01} = 0$ and $r_{03} = 0$, i.e. no edge leaves the source.

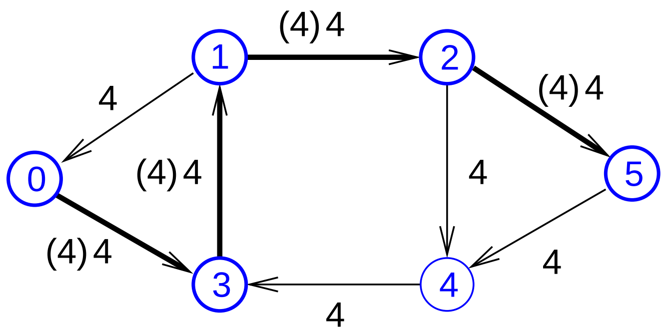

Figure 9: Residual network of small random field system at the second iteration. Now, only one augmenting path exists (highlighted). Again, the values next to the edges denote the residual capacity. The embraced values state the amount of flow which can be pushed along the augmenting path.

This means that no augmenting path exists. Consequently, the maximum flow has been found.

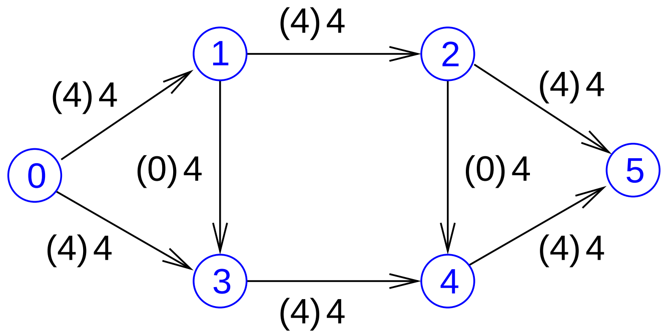

Figure 10: Final flow in network of small random field system. The embraced values state the amount of flow which flows through each edge.

How fast is the Ford-Fulkerson algorithm? Unfortunately it is not possible to find a polynomial in the number of vertices and the number of edges which bounds the time complexity of the method. The reason is that the way an augmenting path is chosen is not determined in any way. The effect of this can be demonstrated by a simple example. Consider the graph in Fig. 11. Assume that the augmenting path is 0,1,2,3 (highlighted). Then the residual capacity of this path is 1, by this amount the flow through the graph is increased. The resulting residual graph is shown in 12. Now an augmenting path is given by 0,2,1,3. Again, the flow is increased by one unit and the flow in Fig. 13 is obtained.

Obviously, by using always this bad choices of the augmenting paths, the Ford-Fulkerson algorithm can be iterated for 10000 times, each time the flow is increased by one unit. On the other hand, it is possible to calculate the maximum flow within two integrations if the augmenting paths 0,1,3 and 0,2,3 are chosen.

This unfavorable behavior is avoided by an extension of the algorithm, which was presented by Edmonds and Karp in 1972 [11]. The basic idea is to chose an augmenting path which has the shortest distance from the source to the sink, where each edge counts with distance one. It can be shown that indeed this algorithm has a polynomial worst-case time complexity of $\Omega(|V||E|^2)$.

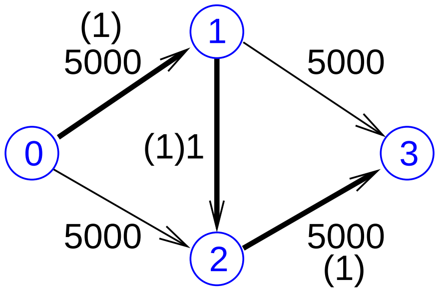

Figure 11: A tiny network where the Ford-Fulkerson Algorithm may spend much time to calculated the maximum flow. Displayed is the residual graph of the first iteration. The resulting flow in the network after the first iteration looks the same.

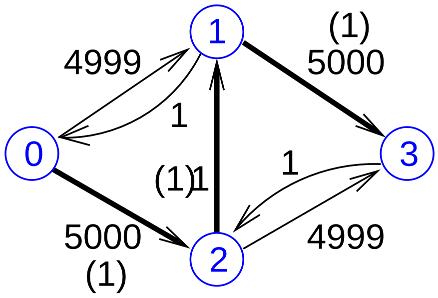

Figure 12: The residual network of the tiny network after one iteration of the Ford-Fulkerson algorithm.

The efficiency of the method of Edmonds and Karp can be further increased by considering many augmenting paths in parallel [15]. A comprehensive description can be found in [13]. An additional speedup can be obtained by applying a method described in [2]. For three-dimensional RFIM systems the corresponding networks can be treated, as found empirically [17], in $\Omega(N^{4/3})$ time, where N is the number of spins.

We have seen that in order to calculate a ground state of a RFIM one has first to construct the corresponding network and then to calculate the maximum flow through the network. *One* minimum cut, which represents a spin configuration of minimum energy, can be found in the following way, which is a special variant of a breadth-first search: the basic idea is to start at the source and to follow only edges where the flow is less than the capacity. The basic idea is one stays always on the left side of the cut, since only edges which are satisfied cross a cut. After all vertices which are accessible from the source in this way have been found, the iteration stops. Then, the spin which have been visited are left to the cut, so they are set to orientation +1, see the definition of $\underline{X}$ in (7) and remember $\sigma_i = 2x_i - 1$. The remaining spins are set to orientation -1.

Please note that in this way only one minimum cut can be obtained, even if several equivalent cuts exists. In the case one is interested in all minimum cuts, one can apply a method explained in [3]. The result is a graph which describes all possible minimum cuts. As example, for the RFIM with bimodal distribution of the random fields the number of cuts (or ground states) grows exponentially with the system size N [17].

Some basic results for RFIM and DAFF can be found in the next section.

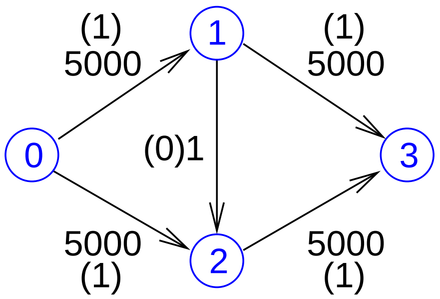

Figure 13: The tiny network after the flow has been increased two times by the Ford-Fulkerson algorithm. The embraced number give the flow through the edges, the other numbers state the capacities of the edges.

4 Results for the RFIM and the DAFF

In this section results of the ground-state calculations for random field systems and diluted antiferromagnet are presented. Mainly the RFIM with bimodal distribution of the random fields is considered. At the beginning the behavior of the order parameter for one realization is presented, then the average results for different system sizes. Using the technique of finite-size scaling, the thermodynamic limit is executed.

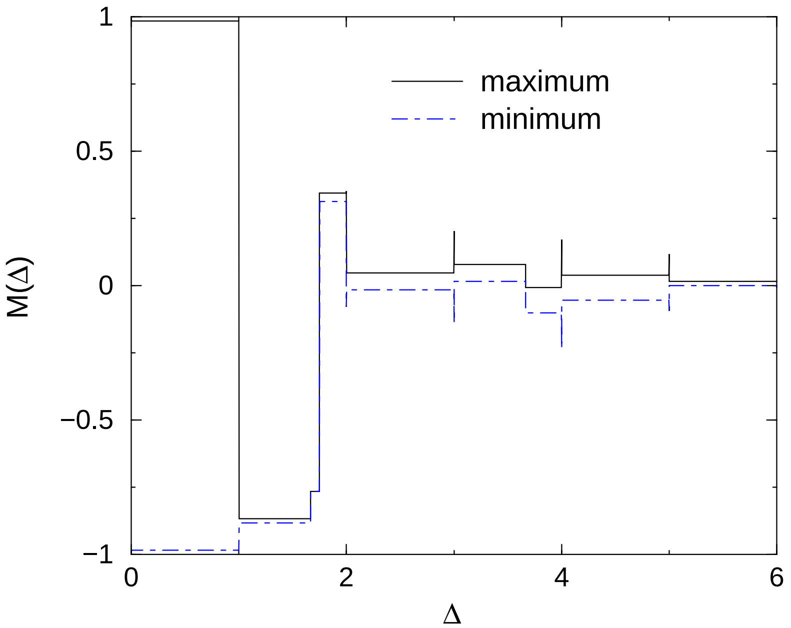

Figure 14: Magnetization M as a function of the strength of the random fields for one realization of a RFIM with bimodal distribution.

In Fig. 14 the behavior of the magnetization $M = 1/N \sum_i \sigma_i$ of one small $N = 8^3$ realization of a random field system with bimodal distribution of the fields is shown. Since this kind of systems exhibit a ground-state degeneracy, the magnetization may vary from one ground state to the other. In the figure the extreme values the magnetization can take are shown. But this does not mean that intermediate values occur always. For very small fields the ground state is only two-fold degenerate: one ground-state is the inversion of the other, thus the magnetization just changes its sign. In general, the behavior turns out to be as expected in the first section: for small fields the system is ferromagnetically ordered. With increasing strength of the random fields the spins tend to be oriented in the direction of the local fields and the magnetization vanishes. The order parameter changes only at a finite number of values for Δ, in between it is constant. A detailed analysis [17] shows that the steps in $m(\Delta)$ occur whenever the sum of local fields on some cluster is strong enough to flip the whole cluster.

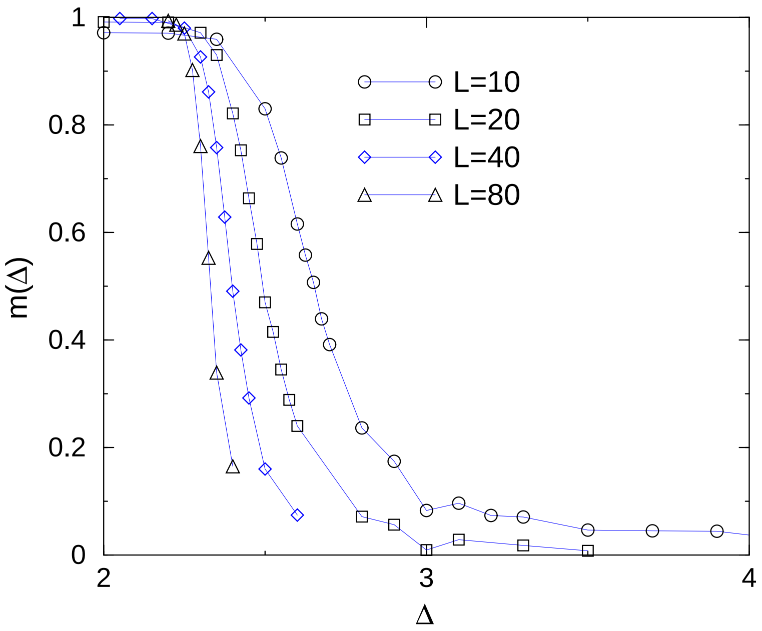

Figure 15: Average maximum of the absolute value of the magnetization as a function of the strength of the random fields. An averaged for 1000 realizations of the RFIM with bimodal distribution was taken. Lines are guide to the eyes only.

The behavior is similar for other realizations, but the values where the cluster turn around vary from system to system. Only the jump at integer values of Δ appear in all realizations. These discontinuities are due to the reversing of several single spins. By averaging over different realization the jumps smear out. The result is shown in Fig. 15 for the maximum of the absolute value of the magnetization averaged over typically 1000 different realizations. For other quantities like the minimum or the average of the magnetization the results look similar. In the figure the data for 4 different system sizes $N = 10^3$, 20^3, 40^3 and 80^3 is presented. With increasing system size a monotonic shift of the curves can be observed. We are interested in performing the thermodynamic limit, i.e. in obtaining the behavior of very large systems. This can be done by applying the technique of finite-size scaling. The basic assumption is that the average magnetization shows the following behavior [20]:

$$m = L^{-\beta/\nu} \tilde{m} \left((\Delta - \Delta_c) L^{1/\nu} \right) . \tag{21}$$

Δ_c is the critical value of the infinite system where the magnetization vanishes. The values of the critical exponents β and ν describe the asymptotic behavior of the order parameter respectively the correlation length near the transition. The exact for of the function $\tilde{m}$ is unknown in general. The values for Δ_c, ν and β have to be determined. They can be obtained by rescaling the numerical data in a way that all data point collapse onto one curve. The resulting *scaling plot* is shown in Fig. 16. The values obtained in this way are $\Delta_c = 2.20$, $\nu = 1.67$ and $\beta = -0.01$.

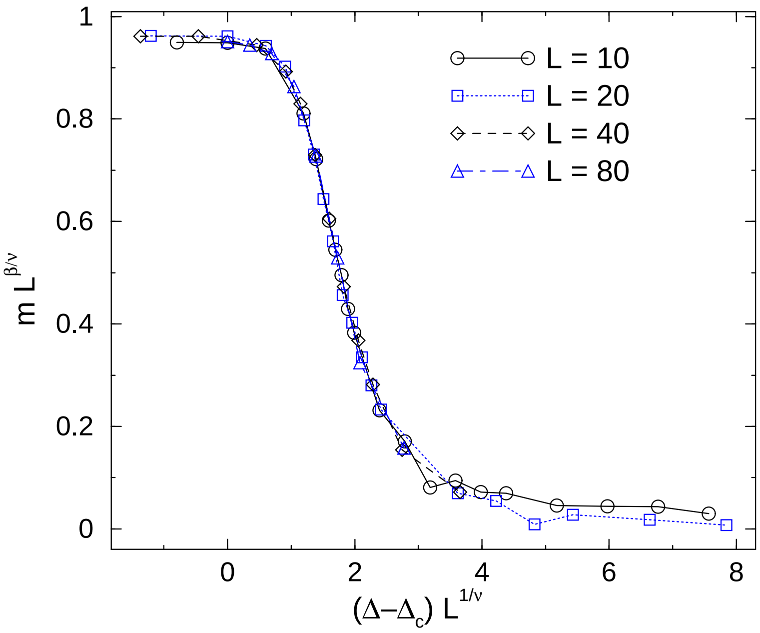

Figure 16: Finite-size scaling plot for RFIM with bimodal distribution. The parameters are $\Delta_c = 2.20$, $\nu = 1.67$ and $\beta = -0.01$

As mentioned at the beginning, it is assumed that the RFIM is similar to the DAFF. In this case the values for the exponents should be equal. Additionally, they should not depend on details of the model like the choice of the distribution of the random fields. In this case one says that the exponents are *universal*. On the other hand, the exact value of the critical strength of the field is not expected to be universal. By calculating similar finite-size scaling plots for the RFIM with Gaussian distribution and the DAFF, the following values are found:

- Gaussian RFIM: $\Delta_c = 2.29$, $\nu = 1.19$ and $\beta = 0.02$
- DAFF: $\Delta_c = 0.62$, $\nu = 1.14$ and $\beta = 0.02$

Consequently, the exponents seem to be not universal, since ν is different for the different distributions of the RFIM. On the other hand, the Gaussian random field system seems to be a good model for diluted antiferromagnets, since in this case the values of the exponents agree.

References

[1] A.K. Hartmann and K.D. Usadel, Physica A **214** (1995), 141.

[2] J.L. Träff, Eur. J. Oper. Res. **89**, 564 (1996)

[3] J.-C. Picard and M. Queyranne, Math.Prog.Study **13**, 8 (1980)

[4] K.D. Usadel and U. Nowak, JMMM **104-107**, 179 (1992)

[5] U. Nowak and K.D. Usadel, Phys. Rev. B **44**, 7426 (1991)

[6] M.N.S. Swamy and K. Thulasiraman, Graphs, Networks and Algorithms (Wiley, New York 1991).

[7] J.D. Claiborne, Mathematical Preliminaries for Computer Networking (Wiley, New York, 1990).

[8] W. Knödel, Graphentheoretische Methoden und ihre Anwendung (Springer, Berlin, 1969)

[9] J.-C. Picard and H.D. Ratliff, Networks **5**, 357 (1975)

[10] L.R . Ford, D.R. Fulkerson, Canadian J. Math. **8**, 399 (1956)

[11] J. Edmons and R.M. Karp, J. ACM **19**, 248 (1972)

[12] L.R. Ford and D.R. Fulkerson, Flows in networks, Princeton University Press, Princeton 1962

[13] R.E. Tarjan, Data Structures and Network Algorithms, Society for industrial and applied mathematics, Philadelphia 1983

[14] L. Schrage, K.R. Baker, Oper.Res. **26**, 444 (1978)

[15] Soviet Math. Dokl. **11**, 1277 (1970)

[16] C. Frontera and E. Vives, Phys. Rev. E **59**, R1295 (1999)

[17] A.K. Hartmann, Physica A **248**, 1 (1998)

[18] A.K. Hartmann and U. Nowak, Eur. Phys. J. B **7** , 105 (1999)

[19] E.T. Seppälä, V. Petäjä, and M.J. Alava, Phys. Rev. E **58**, R5217 (1998)

[20] K. Binder and D.W.Heermann, Monte Carlo Simulation in Statistical Physics, Springer, Heidelberg 1988